U.S. DEPARTMENT OF ENERGY | Office of Science

DOE/SC-ARM-TR-315

SAIL Radar b1 Data Processing: Corrections, Calibrations, and Processing Report

A Matthews
E Schuman
M Rocque
M Deng
Y-C Feng

January 2025

ARM

DISCLAIMER

DOE/SC-ARM-TR-315

SAIL Radar b1 Data Processing: Corrections, Calibrations, and Processing Report

A Matthews
M Deng
E Schuman
Y-C Feng
M Rocque
All at Pacific Northwest National Laboratory

January 2025

How to cite this document:

Matthews, A, M Deng, E Schuman, Y-C Feng, and M Rocque. 2025. SAIL Radar b1 Data Processing: Corrections, Calibrations, and Processing Report. U.S. Department of Energy, Atmospheric Radiation Measurement user facility, Richland, Washington. DOE/SC-ARM-TR-315.

Work supported by the U.S. Department of Energy,
Office of Science, Office of Biological and Environmental Research

Acknowledgments

This research was primarily supported by the Office of Biological and Environmental Research of the U.S. Department of Energy as part of the Atmospheric Radiation Measurement (ARM) user facility, an Office of Science facility.

Acronyms and Abbreviations

AMF	ARM Mobile Facility
ARM	Atmospheric Radiation Measurement
CSU	Colorado State University
DSD	drop size distribution
eRCA	extended radar relative calibration adjustment
GE	general mode
KAZR	Ka-band ARM Zenith radar
LDQUANTS	Laser Disdrometer Quantities Value-Added Product
MD	moderate mode
PPI	plan position indicator
Py-ART	Python ARM Radar Toolkit
RF	radio frequency
SAIL	Surface Atmosphere Integrated Field Laboratory
SNR	signal-to-noise ratio
VDISQUANTS	Video Disdrometer Value-Added Product
WRA	wet radome attenuation
XPRECIP	scanning X-band precipitation radar

Contents

Figures

Tables

1.0 Introduction

The U.S. Department of Energy (DOE) Atmospheric Radiation Measurement (ARM) user facility deployed the second ARM Mobile Facility (AMF2) near Crested Butte, Colorado for the Surface Atmosphere Integrated Field Laboratory (SAIL) campaign. The SAIL campaign occurred from September 1, 2021, to June 15 2023.

To study the water cycle in the East River Watershed, ARM deployed a vertically pointing Ka-band ARM Zenith radar (KAZR) and a scanning X-band precipitation radar managed by Colorado State University (CSU XPRECIP), as shown in Figure 1.

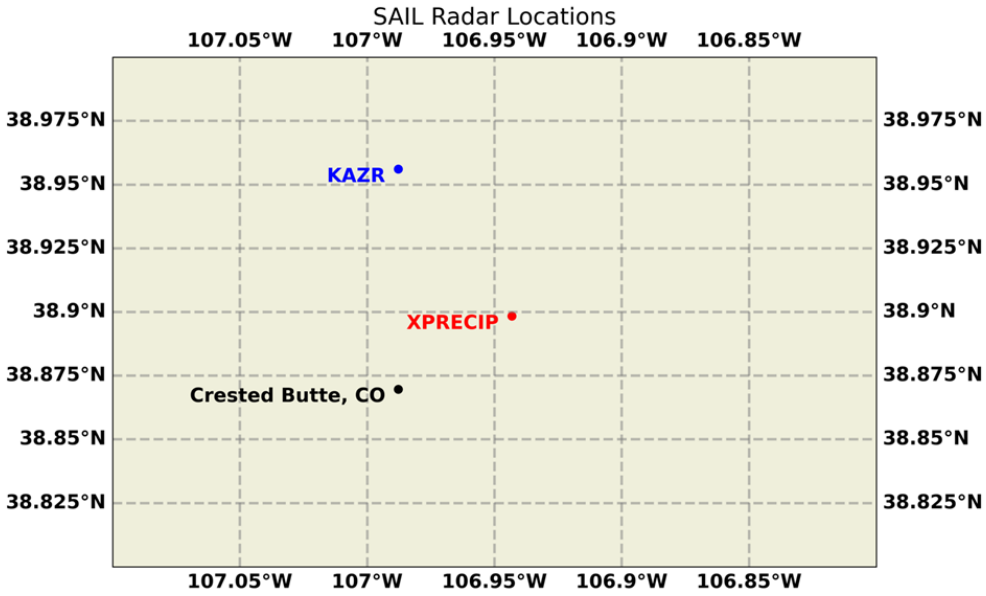

Figure 1. Radar locations during SAIL.

1.1 Overview of SAIL Radars

Table 1 shows the specifications of the KAZR and XPRECIP radars. As the XPRECIP was managed by CSU, calibrations and corrections to this data were provided by CSU and are noted in this table as well. The radars can be seen in Figure 2.

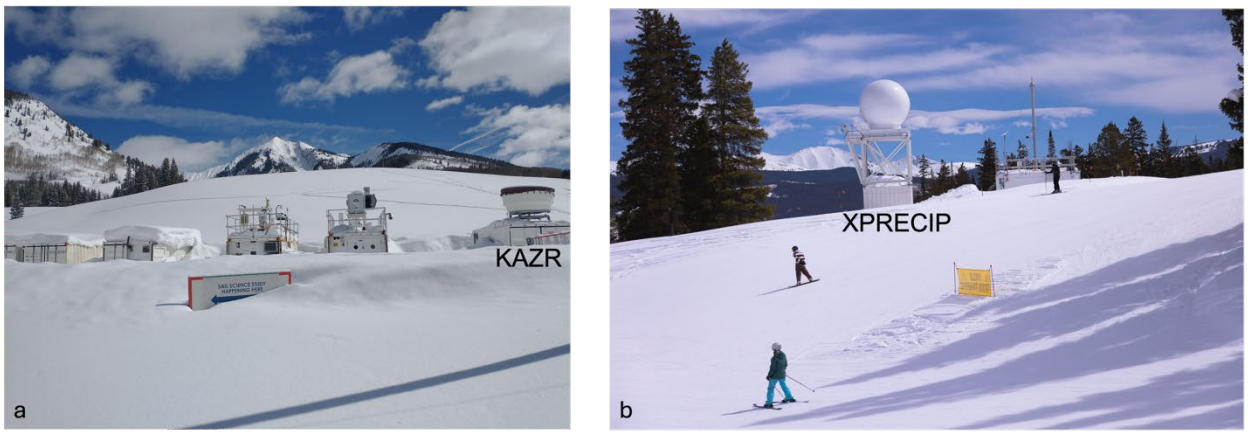

Figure 2. Images of the KAZR (a) and XPRECIP (b) during the SAIL field campaign.

Table 1. Radar specifications during the SAIL field campaign.

Radar	Frequency (GHz)	Wavelength (mm)	Transmit power (kW)	Antenna diameter (m)	Beam width (deg)	Gate spacing (m)	Polarization
KAZR	34	8.57	0.187	2	0.3	29.98	Single

1.2 Overview of b1 Processing

As shown in the previous b1 reports, b1 processing is an activity that typically focuses on using only a single instrument, although comparisons with other instruments may be done. This section will cover the steps taken for the SAIL radar corrections at a high level, before describing each step in more detail. Although both the KAZR and XPRECIP were deployed by ARM for this campaign, only the data quality and corrections for the KAZR will be discussed in this report, as the XPRECIP corrections were done by Dr. Chandra's research group at CSU. A flow chart of b1 efforts is shown in Figure 3.

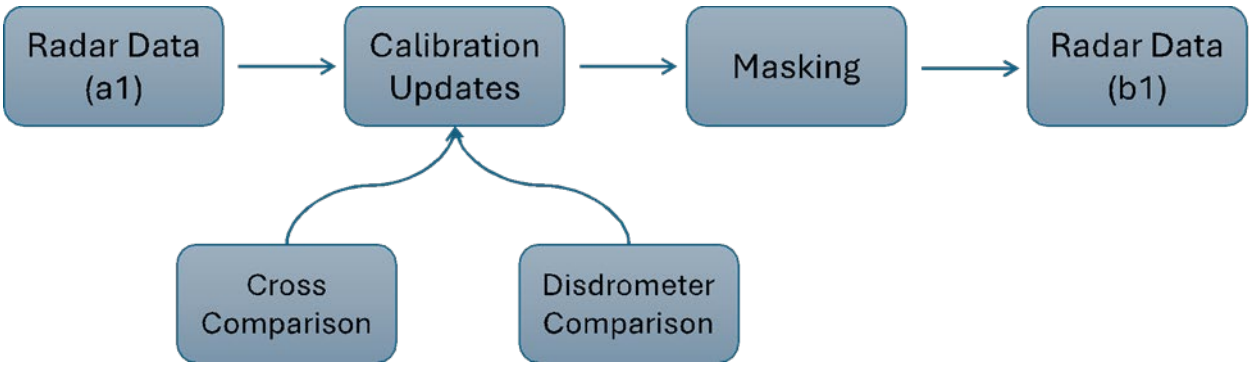

Figure 3. Radar b1 computational flowchart for SAIL.

1.2.1 Calibration

The primary purpose of the b1 processing is the calibration of the radar datastreams. The calibration of a radar can drift in a variety of ways. The primary function of calibration is to fix the value of the radar constant, C. This constant affects nearly all power measurements the radar takes and represents one of the most dominant sources of errors for the radar. Fundamentally, the radar constant is used as:

$$Z(ri) = P(ri) - C + 20*10\ (ri)$$

The radar constant C is made up of numerous terms including the finite filter loss, the gain of the antenna, and the wavelength. We can, however, represent it as a constant. Once the constant is solved for, correcting calibration is a linear operation for a given time step. This calibration constant as defined exists for all radars. In the case of the KAZR, where pulse compression is used, a separate radar constant is required for each radar mode. Note that the calculations are not always constant in time, as the transmitted radar power, the waveguide loss, and other factors may drift with environmental and/or radar stability changes.

SAIL calibrations posed new challenges when compared with the previous efforts because there were fewer ARM radars deployed for cross-comparisons, and the winter precipitation limited time periods where comparisons with disdrometers could be completed. The winter precipitation and remote location also lead to build up of snow and ice on the radome.

1.2.2 Data Quality Masks

The radars measure not just hydrometeors, but are also sensitive to ground clutter, sea ice, sea clutter, insects, and extraneous radio frequency (RF) interference. To make the data more useable, masks that separate the hydrometeors from these non-meteorological signals are provided. This mask does not mean the data is “bad”, but rather to provide an estimate of where the meteorological data is located. Because the processing and measured parameters vary for each radar, the masks available for each datastream will also vary.

1.2.3 Data Quality Corrections

In addition to calibration and data quality masks, other circumstances may cause poor quality radar data. Sometimes, these issues (e.g., complete power/site outage) are not correctable, but several issues can be remedied. Wherever possible, b1 efforts correct for malfunctions or misconfigurations of the radar (e.g., as may still be found in a1 or b0 files). When a correction cannot be provided, data quality notes are appended to those data sets and/or described further in this report.

1.3 Radar Performance

The operational periods for the KAZR and XPRECIP columns over the KAZR during SAIL are shown in Figure 4. The KAZR operations were very stable throughout the campaign. The XPRECIP had a few small data outages, but overall also operated consistently during SAIL. All a1- and b1-level data can be downloaded from the ARM Data Discovery tool, and plots from the a1-level data may be viewed on the ARM DQPlotbrowser.

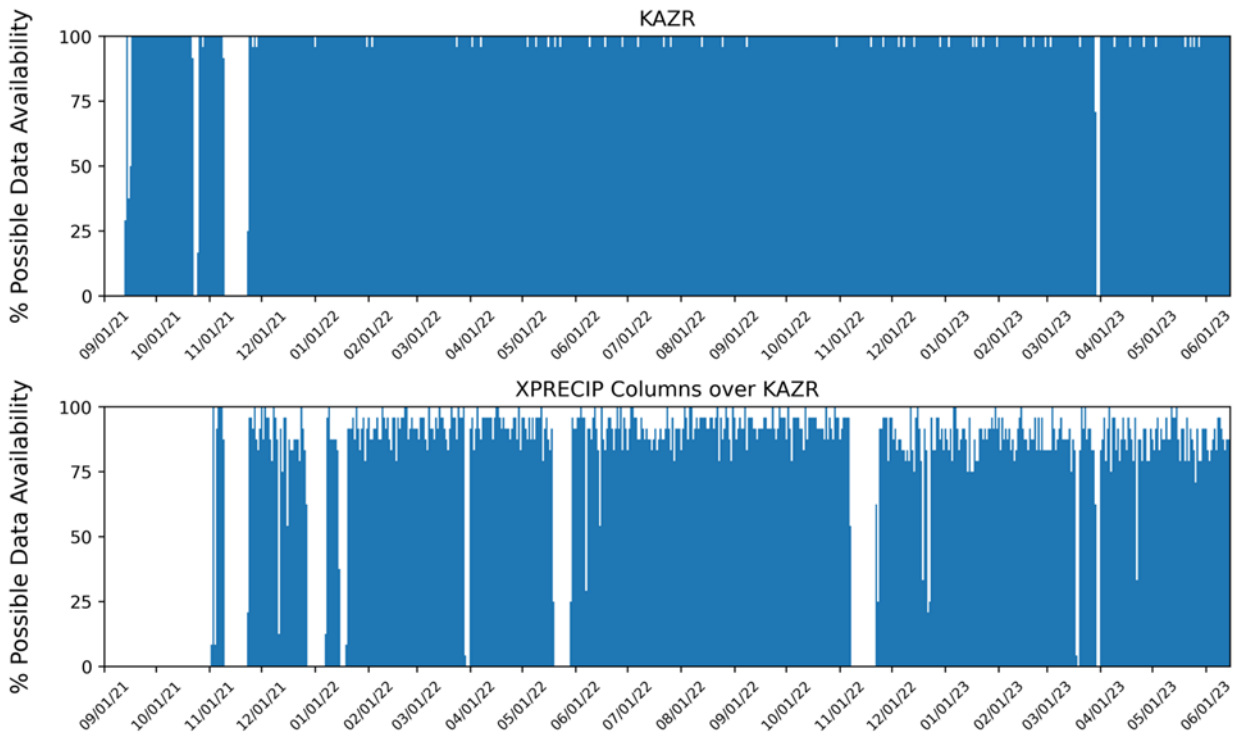

Figure 4. Radar data availability per day, as a percentage of expected operations.

2.0 Calibrations and Corrections

The calibration of the radars is a multi-part processing consisting of tasks including onsite measurements as well as post-campaign data analysis such as cross-comparisons with other radars in the area. As this report focuses solely on the KAZR calibrations, certain techniques used in past ARM b1 calibration such as corner reflector scans and extended radar relative calibration adjustment (eRCA) were unable to be implemented. Additionally, comparisons with disdrometers were only conducted during times of liquid precipitation. Therefore, radar calibrations during SAIL are based on relative calibration through radar cross-comparisons and summer disdrometer comparisons.

2.1 Techniques

Several techniques are used to calibrate and correct reflectivity-based variables. The following subsections describe the techniques and how they are applied to the radars.

2.2 KAZR Corrections

The KAZR operates using two different pulses, called its “GE” and “MD” modes. The first, GE or general mode, is a short pulse that provides returns near the ground and is sensitive to most cloud types. The second, MD or moderate mode, is a longer chirped pulse that provides a higher level of sensitivity, so it is more capable of seeing thinner clouds such as cirrus. However, the MD mode does have a large blind

range than GE mode because it cannot 'see' while it is transmitting, so misses the first 800 m above the radar.

This KAZR is single polarization, so calibration focused on these two pulse modes reflectivity only. To achieve this, we compared the KAZR GE-mode reflectivities to the XPRECIP reflectivities to see a relative offset. We also used a disdrometer comparison using a wet radome attenuation (WRA) method to find differences between the KAZR reflectivity and disdrometer calculated reflectivity that are not affected by water accumulating on the KAZR radome. Comparisons between the GE and MD modes were also completed.

2.2.1 Cross-Comparisons with XPRECIP

2.2.1.1 XPRECIP Data Quality

As we showed previously, the XPRECIP operated well throughout the SAIL campaign. Dr. Chandra's research team at CSU supplied this radar for SAIL, and therefore also were responsible for maintenance during the campaign and data quality corrections. They performed multiple checks, including comparisons with disdrometers and direct hardware measurements, which showed that they suggested a 2 dB addition to reflectivity.

During the campaign, the XPRECIP had an outage due to a computer problem starting November 7 2022 and returned to consistent operations on November 24 2022. After this outage, there was a change in the background reflectivity of the XPRECIP radar, as shown in Figure 5.

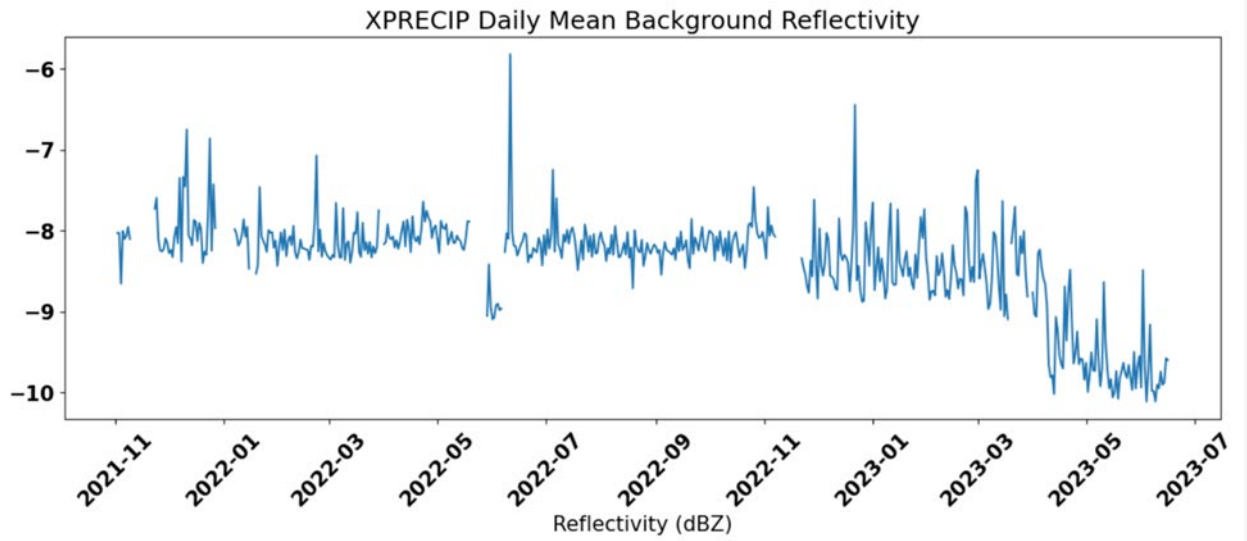

Figure 5. Daily mean background reflectivity for the CSU XPRECIP radar, showing a change in November 2022 and again in March 2023.

2.2.1.2 XPRECIP and KAZR GE Comparisons

One method used to arrive at the KAZR GE reflectivity correction was to compare with the XPRECIP radar after the correction mentioned in the previous section had been applied. To compare the vertically

pointing KAZR with the scanning XPRECIP radar, columns were created from the XPRECIP radar over the location of the KAZR using the Python ARM Radar Toolkit (Py-ART). The scan strategy for the XPRECIP plan position indicator (PPI) data can be seen in Figure 6.

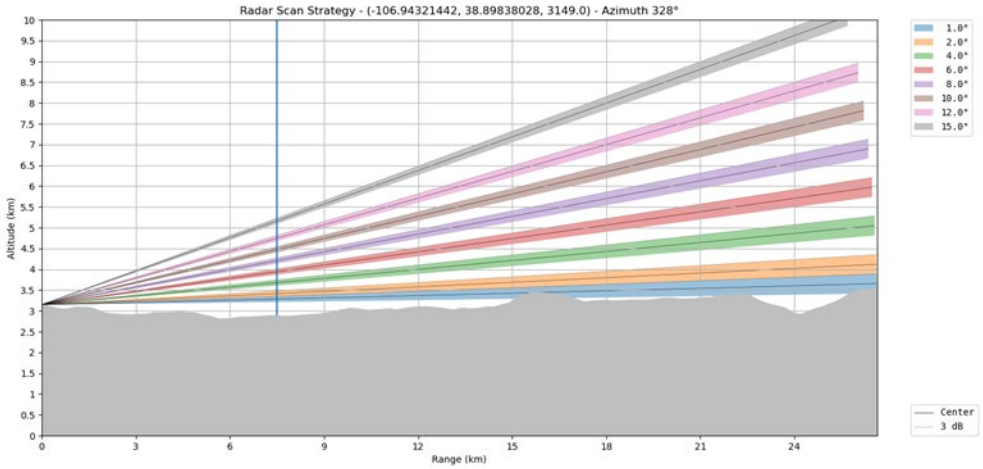

Figure 6. PPI scan elevations for the XPRECIP radar during SAIL. The KAZR location is shown in a vertical blue line.

These columns were then filtered so only data below 2 km above ground with signal-to-noise-ratios (SNR) above 0, a correlation coefficient (RhoHV) above 0.9, and reflectivities between -5 and 15 dB were used for comparison. This ensured we were comparing similar clouds with less impact from attenuation. Once this was complete, the data were filtered again to only include hours with rain rates of less than 0.01 mm/hr. This was included to again mitigate any effect from attenuation through the clouds, but also because water may collect on the KAZR radome during moderate to high rain rates that can lead to upwards of 10 dB of additional offset that is unrelated to any systematic biases. The comparison between the XPRECIP and KAZR reflectivities using these filters can be seen in Figure 7. The mean offset in the first half of the campaign is around 0.5 dB, while after the November 2022 XPRECIP outage the offset is around -3 dB. This comparison may be affected by attenuation as the XPRECIP was located 7.5 km from the KAZR and may have some errors caused by snow buildup on the radome.

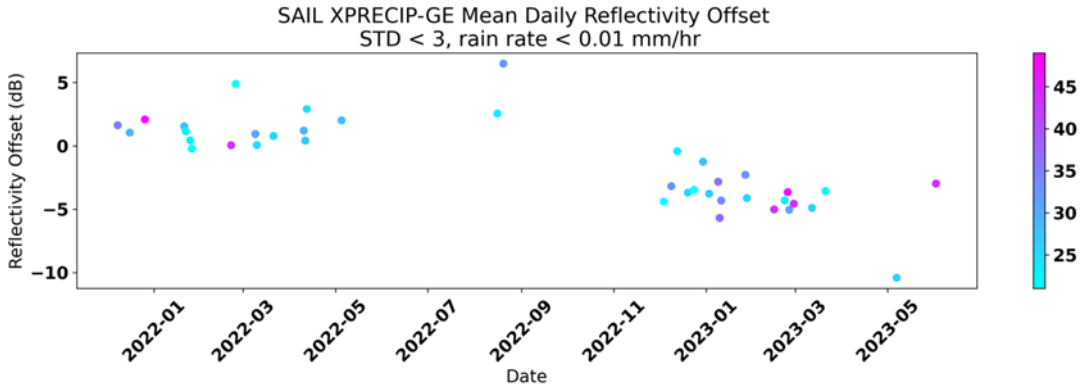

Figure 7. Comparison between XPRECIP and GE reflectivities during times of very light or no rain.

2.2.2 Comparisons with Drop Size Distribution (DSD)

2.2.2.1 Wet Radome Attenuation Relative Calibration Technique

The difference between the KAZR measured and ARM's Laser Disdrometer Quantities (LDQUANTS) Value-Added Product estimated Ze from nearby disdrometer measurements is mainly attributed to the radar calibration offset and the WRA. The calibration offset is independent of rain rates, while the WRA, due to the cumulative rainwater collecting on the radar radome, has an intrinsic dependence on rain rates, which is fitted with a log-linear equation for data with rain rates less than 5 mm/hr. The radar calibration offset is then the difference after the WRA correction. Please refer to Deng et al 2024 for more detailed information about the WRA relative calibration technique.

2.2.2.2 KAZR GE and DSD Comparison

KAZR comparisons with a nearby disdrometer were completed for liquid precipitation using the WRA relative calibration technique. The daily difference between the disdrometer and WRA-corrected KAZR GE below 500 m can be seen in Figure 8. This offset was relatively consistent throughout the campaign, with a mean offset of -0.9 dB, with about 2 dB of uncertainty, except the data during May 2023, which may be under the influence of mixed rain and snow in later spring.

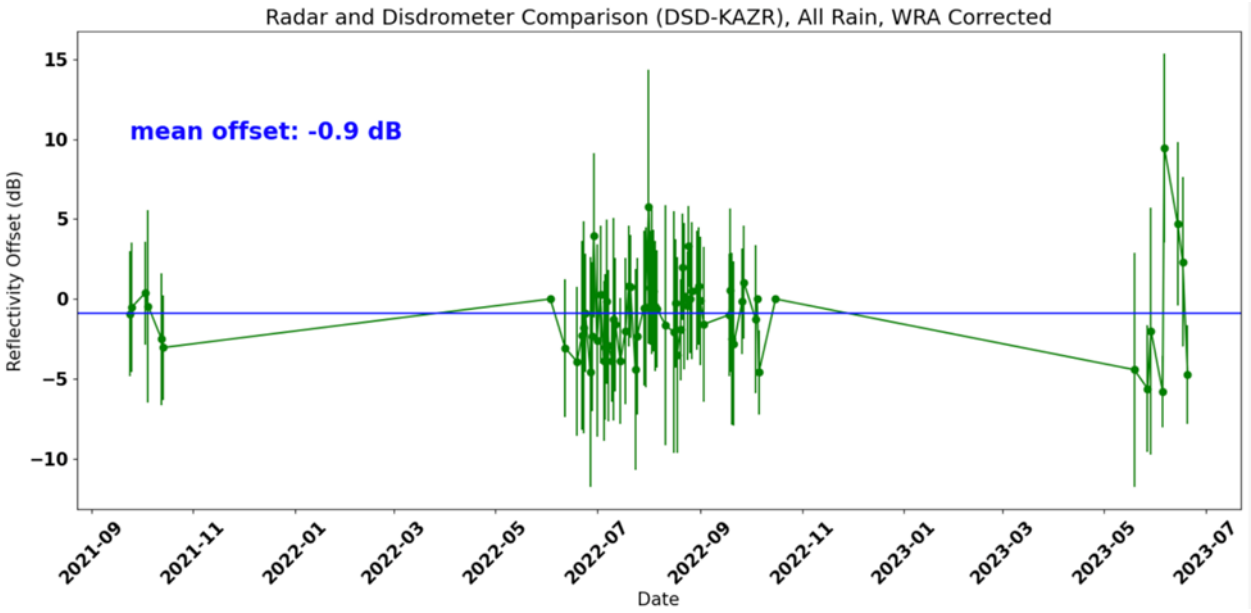

Figure 8. KAZR Ze calibration offset from the WRA relative calibration technique with collocated ARM Video Disdrometer (VDISQUANTS) Value-Added Product data when rain rates are less than 5 mm/hr, showing a mean offset of -0.9 for the campaign.

Based on the consistency of the DSD versus KAZR comparison, and that this offset and the XPRECIP versus KAZR comparison fall within uncertainty of each other, a constant offset of KAZR - 0.9 dB was applied to the full campaign.

2.2.3 KAZR Intermode Comparison

Next, we compared the KAZR GE and MD reflectivities, using a data filter of SNR > 0 dB and reflectivities between -5 and 15 dB to find the MD offset. This also tells us how well the pulse compression filter fits the data throughout the campaign. Figure 9 shows the uncorrected KAZR GE and MD difference of 0.5 dB. The difference is slightly lower during the winter months, which may be due to snow buildup on the radome. Based on this, an offset of -0.5 dB is applied to the KAZR MD mode to correct for the difference between the two modes.

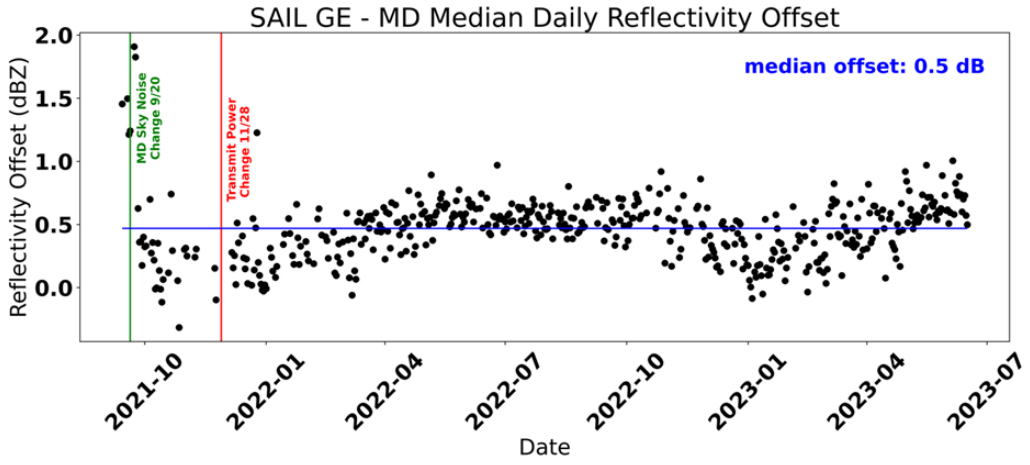

Figure 9. KAZR GE versus KAZR MD, uncorrected reflectivity comparison.

After correction, the GE and MD mode reflectivities agree well as shown in Figure 10, with a mean offset of 0.03 dB.

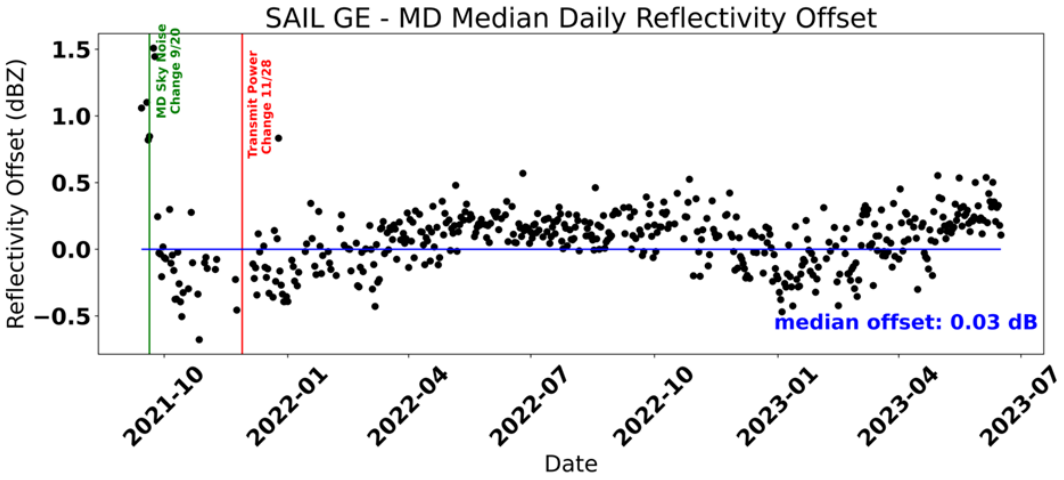

Figure 10. KAZR GE versus KAZR MD, post-correction reflectivity comparison.

3.0 Masks and Post-Processing

3.1 Meteorological Echo Mask

The KAZR GE and MD censor mask uses the texture of the mean doppler velocity field to differentiate between meteorological and non-meteorological echoes. An example of these masks is provided in Figure 11.

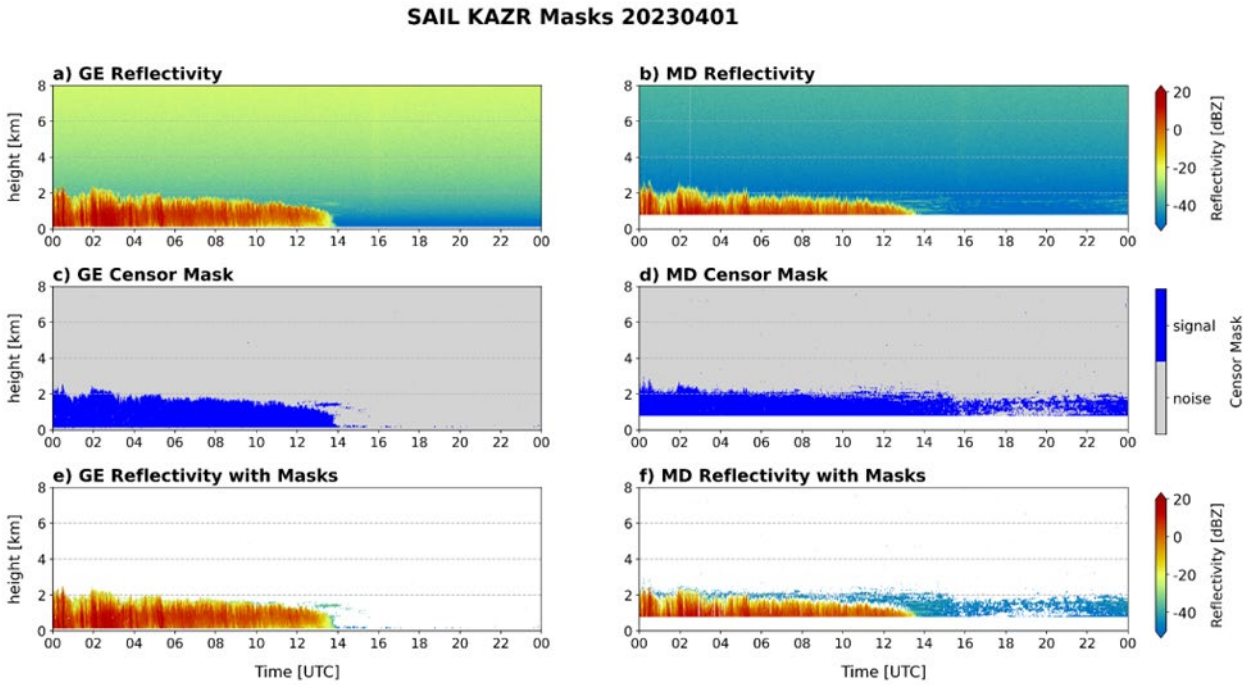

Figure 11. Example case of the masks as applied to the KAZR GE and MD reflectivity data. The raw data is shown in a (ge) and b (md), the censor mask in c (ge) and masked reflectivity data in e (ge) and f (md).

4.0 Description of Data Files

This section contains a description of ***some*** of the more relevant parameters and variables in the radar datastreams.

Table 2. List of the key variables in the b1-level KAZR datastreams.

Key
New variable calculated
Correction applied

KAZR File Contents at b1-level	
Moments	
linear_depolarization_ratio	All values set to nan. This variable is not present in this KAZR.
mean_doppler_velocity	Radial mean Doppler velocity, positive for motion away from the radar.
mean_doppler_velocity_crosspolar_v	All values set to nan. This variable is not present in this KAZR.
reflectivity	Equivalent reflectivity factor, with offset applied.
reflectivity_crosspolar_v	All values set to nan. This variable is not present in this KAZR.
signal_to_noise_ratio_copolar_h	Signal-to-noise ratio (SNR), horizontal channel.
signal_to_noise_ratio_crosspolar_v	All values set to nan. This variable is not present in this KAZR.
spectral_width	Spectral width.
spectral_width_crosspolar_v	All values set to nan. This variable is not present in this KAZR.
Masks	
censor_mask	Bit mask 0: no mask 4: velocity texture threshold of 2.0 applied based on mean_doppler_velocity after correction.

5.0 References

SAIL KAZR image: https://www.flickr.com/photos/armgov/53013652878/in/album-72157719418184231/

SAIL XPRECIP image: https://www.flickr.com/photos/armgov/53020140587/in/album-72157719418184231/

Atmospheric Radiation Measurement (ARM) user facility. 2021. Laser Disdrometer Quantities (LDQUANTS), 2021-09-01 to 2023-06-15, ARM Mobile Facility (GUC) Gunnison, CO; AMF2 (main site for SAIL) (M1). Compiled by J Hardin, S Giangrande, and A Zhou. ARM Data Center. http://dx.doi.org/10.5439/1432694

Chandrasekar, V, L Baldini, N Bharadwaj, and PL Smith. 2014. Recommended Calibration Procedures for GPM Ground Validation Radars, 103. https://gpm-gv.gsfc.nasa.gov/Tier1/Docs/NASA_GPM_GV-cal_9.pdf

Deng M, SE Giangrande, MP Jensen1, K Johnson, CR Williams, JM Comstock, Y Feng, A Matthews, IA Lindenmaier, TG Wendler, M Rocque, A Zhou, Z Zhu, E Luke, and D Wang. 2023. "Calibration of ARM TRACER Cloud Radar Observations Using Disdrometer Measurements under Wet-Radome Conditions." Submitted to *Journal of Atmospheric and Oceanic Technology*.

Hardin J, SE Giangrande, and A Zhou. 2020: Laser Disdrometer Quantities (LDQUANTS) and Video Disdrometer Quantities (VDISQUANTS) Value-Added Products Report. U.S. Department of Energy, Atmospheric Radiation Measurement user facility, Richland, Washington. DOE/SC-ARM-TR-221. https://doi.org/10.2172/1808573

Helmus, JJ, and SM Collis. 2016. "The Python ARM Radar Toolkit (Py-ART), a Library for Working with Weather Radar Data in the Python Programming Language". *Journal of Open Research Software* 4(1): e25, http://doi.org/10.5334/jors.119

Heistermann, M, S Jacobi, and T Pfaff. 2013. "Technical Note: An open source library for processing weather radar data (*wradlib*)." *Hydrology and Earth System Sciences* 17(2): 863–871, https://doi.org/10.5194/hess-17-863-2013

www.arm.gov

U.S. DEPARTMENT OF
ENERGY

Office of Science